Journal of Nano Research Vol. 5 (2009) pp 193-200
online at http://www.scientific.net

Online available since 2009/Feb/06

Synthesis and Photocatalytic Activity of Yb Doped TiO_2 Nanoparticles under Visible Light

Mou Pal[1], U. Pal[2a], R. Silva Gonzalez[2], E. Sanchez Mora[2], and P. Santiago[3]

[1]Posgrado en Ingeniería y Ciencias Aplicadas, UAEM-CIICAP, Av. Universidad 1001, Col. Chamilpa, 62210-Cuernavaca, Morelos, México.
[2]Instituto de Física, universidad Autónoma de Puebla, Apdo. Postal J-48, Puebla, Pue.72570, México.
[3]Instituto de Física, Universidad Nacional Autónoma de México, 01000 México D.F, México.
[a]upal@sirio.ifuap.buap.mx (corresponding author)

Received: October 23rd, 2007; revised: April 15th, 2008; accepted: May 18th, 2008

Keywords: Nanoparticles, Doped TiO_2, Photocatalysis

Abstract. Developing new semiconductor materials with improved photocatalytic activity is a promising technology for the remedy of environmental pollution. Here we report on the synthesis of Yb containing TiO_2 nanoparticles and their catalytic activity under visible light. Highly monodispersed, spherical TiO_2 and TiO_2 :Yb nanoparticles of 27- 40 nm size range were prepared through controlled hydrolysis of titanium tetrabutoxide (TTB) and characterized by X-ray diffraction (XRD), energy dispersion spectroscopy (EDS), high-resolution transmission electron microscopy (HRTEM), high angle annular dark field (HAADF), and ultraviolet-visible diffuse reflectance spectroscopy (UV-vis DRS) techniques. Average size of the nanoparticles was found to decrease with the increase of Yb doping concentration. The photocatalytic activity of Yb doped TiO_2 was evaluated by measuring the degradation rates of methylene blue (MB) under UV and visible lights. Doping with ytterbium ions enhanced significantly the photocatalytic activity of TiO_2 nanoparticles for MB oxidation under visible light.

Introduction

Development of nanostructured materials with tailored physical and chemical proprerties for advanced technological applications is one of the challenging issues for the materials scientists today. TiO_2 is considered as the most efficient and environmentally benign photocatalyst and has been widely used for photodegradation of organic pollutants [1,2]. Most of the investigations in this area were focused on the use of nanosized TiO_2 in order to improve its light absorption capacity. The high surface to volume ratio of the nanostructures also enhances their catalytic activities. Rutile, anatase and brookite are the well known naturally occuring TiO_2 polymorphs which differ to each other in chemical as well as physical properties. Under ambiental conditions rutile is thermodynamically more stable than anatase or brookite. However, thermodynamic stability is particle-size dependent and at average diameters below 14 nm, anatase is the more stable phase than rutile [3]. Anatase, having a band gap of 3.2 eV, has the highest photocatalytic activity due to its higher degree of hydroxylation, slightly higher Fermi level and lower capacity of adsorbing oxygen [4-6]. Nevertheless, many applications of TiO_2 are hindered to some extent by its wide band gap. The band gap of bulk TiO_2 lies in the UV regime (3.0 eV for rutile phase and 3.2 eV for anatase phase), that implies only a small fraction of solar spectrum (<10%) can be utilized effectively. Another limiting factor for widespread use of TiO_2 as photocatalyst is its relatively high electron-

hole recombination rate [7]. In photocatalysis, the electron-hole (e^-/h^+) pairs generated by photon excitation participate in redox reactions on particle surface. In TiO_2, the rate of e^-/h^+ pair production and their subsequent recombination are faster than the rates at which the electrones and holes are trapped and participate in redox reactions [8-9]. Obviously, the electron and hole recombination process is detrimental to the efficiency of a semiconductor photocatalyst, and needs to be retarded for an efficient charge transfer process to occur on the photocatalyst surface. Charge carrier trapping could suppress recombination and increase the lifetime of the separated electrone and hole [10]. Chemical modification of TiO_2 nanomaterials with dopants can alter the charge-transfer properties, which, in some cases is beneficial to their photocatalytic performance. In order to extend its absorption edge into the visible region, many attemts have been made including dye sensitization [11], external surface modifications [12] and band gap tailoring by doping with transition metals [13,14], nonmetallic elements [15-17] and rare earth ions [7,9,18,19]. In this article we describe a room temperature synthesis of Yb doped TiO_2 nanoparticles and their photo-catalytic performance. The catalytic activity of the nanostructures was evaluated by measuring the degardation rates of methylene blue both under ultraviolet and visible light. Effect of Yb doping on the enhancement of MB photodegradation is discussed.

Experimental characterization

Synthesis

In a typical synthesis, 2.5 ml of titanium (IV) *n*-butoxide ($Ti(OBu)_4$, Sigma Aldrich, 97%) was added to 25 ml of anhydrous ethanol (Baker) in nitrogen atmosphere and was agitated at room temperature for 25 min. The resulting transparent solution was added dropwise to 150 ml of deionized water (E-pure Barnstead system, 18.0 MΩ cm) which was adjusted previously to a pH of 3.8 using 0.1 M nitric acid. White precipitate of TiO_2 was immediately formed in the mixture solution, which has been separated and washed by centrifugation. For Yb doping, required amounts of $YbCl_3.6H_2O$ (Alfa-Aesar) corresponding to nominal 0.5, 2 and 8 mol % doping level were added to the deionized water before adjusting its pH. The as prepared samples were annealed at 550 ^{0}C for 2h in N_2 atmosphere in a tubular furnace.

XRD, EDS and TEM characterization

X-ray diffraction data of the samples was collected using an X'Pert Philips diffractometer using Cu-Kα (λ = 1.5406 Å) radiation. The composition of the samples was estimated through energy dispersive spectroscopy (EDS, Thermo Noran SuprDry analytical system). A JEM 2010 Fas Tem electron microscope with 0.19 nm resolution (point to point) equipped with a Z-contrast scanning transmission electron microscopy (STEM) using high angle annular dark field (HAADF) detector and energy filtered TEM (EFTEM) unit was used for structural characterization. The resolution in HAADF-STEM modes was of the order of 0.2 nm. The XRD patterns for doped and undoped samples are given in figure 1. All the diffraction peaks could be assigned to pure anatase phase [20] without any ambiguity. It should be noted that with the increase of Yb doping concentration, the diffraction peaks are broadened, suggesting a systematic decrease in the grain size for the samples. Moreover, a gradual shift in peak position for the (101) peak towards lower angles is observed with the increase of Yb content, suggesting the deformation of crystalline lattice. This result is analogous to that reported in the literatures [21, 22]. The peaks correspond to the crystal planes (101) and (200) are selected to determine the lattice parameters of Yb doped and undoped TiO_2 samples. The lattice parameters are calculated using the equations:

$$d_{(hkl)} = \lambda / 2 \sin\theta \quad \text{(Bragg's law), and}$$

$$d_{(hkl)} = (h^2/a^2 + k^2/b^2 + l^2/c^2)^{-1/2}$$

where *hkl* are the Miller indices, *a, b* and *c* are the lattice parameters (in tetragonal structure, $a = b \neq c$); and d_{hkl} is the interplaner spacing between the crystal planes (*hkl*). λ is the X-ray wavelength and θ is the diffraction angle of the crystal planes *(hkl)*. The estimated lattice parameters and cell volume for the samples are summarized in table 1. Increased lattice distortion with increasing doping concentration is clear, which is conceivable from the quite big size discrepancy between Ti^{+4} (0.605 Å) and Yb^{+3} (0.860 Å) ions.

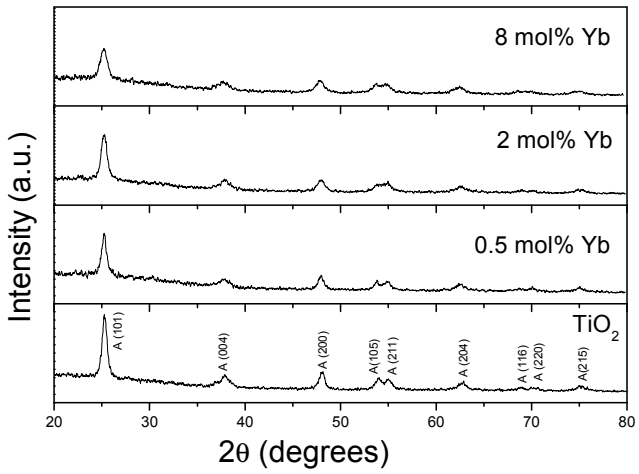

Figure 2a. X-ray diffraction patterns for TiO_2:Yb with 0, 0.5, 2.0, and 8.0 mol% of Yb doping.

Table 1. Lattice parameter and unit cell volume of the Yb doped and undoped TiO_2 nanostructures.

Samples	a = b [Å]	c [Å]	Cell volume [Å^3]
TiO_2	3.778	9.7404	139.02
0.5 mol% Yb	3.7908	9.4915	136.39
2 mol% Yb	3.7917	9.5346	137.07
8 mol% Yb	3.8020	9.5782	138.45

The morphology and size of the TiO_2 nanocrystals were studied by transmission electron microscopy. Formation of spherical TiO_2 nanoparticles of sizes ranging from 41 to 27 nm is clear from the TEM images (Fig. 2). From the size distribution histograms presented in figure 2, it can be seen that the average size of the particles decreases with the increase of doping concentration. As the ionic radius of Yb is considerably bigger than that of Ti, the growth of TiO_2 nanocrystallites was hindered by Yb doping [23]. The composition of the samples was estimated through EDS measurements. The results of EDS elemental analysis are presented in Table 2. Apart from the emission peaks of Ti, O and Yb, the peaks of C and N were also observed in the spectra (Fig. 3). Nitrogen was probably incorporated in the samples during sintering in nitrogen atmosphere, and C might have come from the carbon tape used to prepare the samples for EDS measurements. The EDS estimated Yb concentrations for the nominal 0.5, 2 and 8 mol % doped [calculated by [Yb]/[Ti] x 100%] samples were 0.80, 0.87 and 0.97 atom %, respectively. The concentration of Ti reduced from 40.46 atom % in undoped TiO_2 to 36.71 atom % in 8 % doped sample. The increase of Yb concentration in the samples caused a systematic decrease of titanium concentration indicating the replacement of Ti atoms by Yb in TiO_2 lattice.

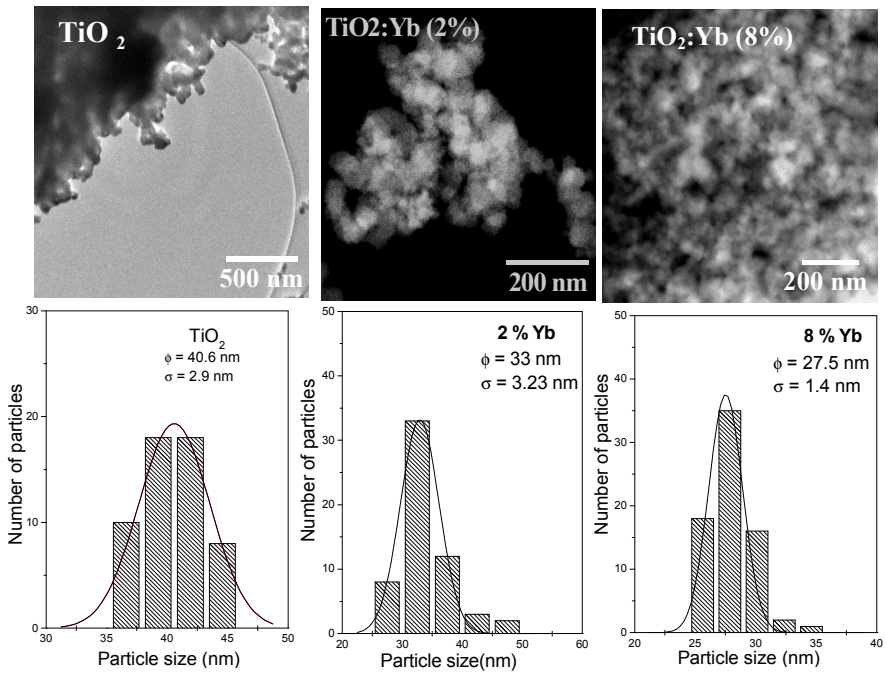

Figure 2. Typical TEM images of undoped and doped TiO_2 nanoparticles (top) with corresponding particle size distribution histograms (bottom).

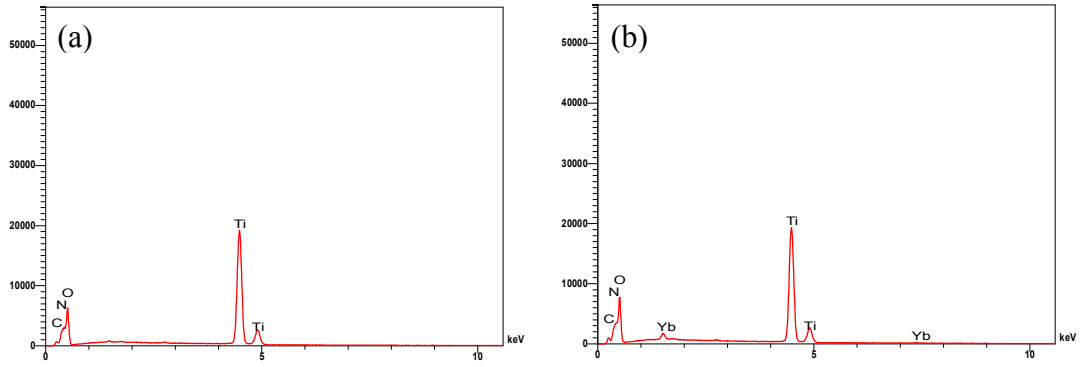

Figure 3. EDS spectra for (a) undoped, and (b) 8% Yb doped TiO_2 nanoparticles.

Table 2. EDS estimated elemental composition for undoped and doped TiO_2 nanoparticles.

Sample	Atomic %		
	Ti	O	Yb
Undoped TiO_2	40.46	59.54	0
Yb 0.5 mol %	38.02	61.18	0.80
Yb 2 mol %	37.24	61.89	0.87
Yb 8 mol %	36.71	62.32	0.97

The existence of lattice distortion caused by Yb doping was further confirmed from the HRTEM results (Fig. 4). While the undoped TiO_2 exhibited clear, well defined crystalline planes without any deformation, the 8% Yb doped sample showed highly distorted lattice planes with larger *d* values and lower crystallinity compared to undoped TiO_2 sample. Figure 5 shows the

HAADF-STEM image of 8% Yb doped TiO_2 nanoparticles. When the particles of interest contains heavy elements, high-angle annular dark field scanning TEM (HAADF-STEM) is the right choice to determine their existence in the matrix, as the contrast of the HAADF image is strongly related with the atomic number of the elements [23]. Inhomogeneous bright contrast of the HAADF image presented in figure 5 clearly revealed the inhomogeneous distribution of Yb in the 25-30 nm TiO_2 nanoparticles. Apparently, the incorporated Yb remained in the TiO_2 matrix as small clusters. To investigate the distribution of Yb in TiO_2 matrix, elemental mapping using EFTEM was performed on some selected area of the 8% Yb doped sample (Fig. 6). EFTEM is considered as an important tool for mapping elemental distributions. Inhomogeneous distribution of Yb in TiO_2 nanoparticles is very clear from the EFTEM images of figure 6, where Yb N-edge (185 eV) was selected for energy filtering. Presence of Yb in higher concentrations at the boundary of the particles is clearly observed in the images.

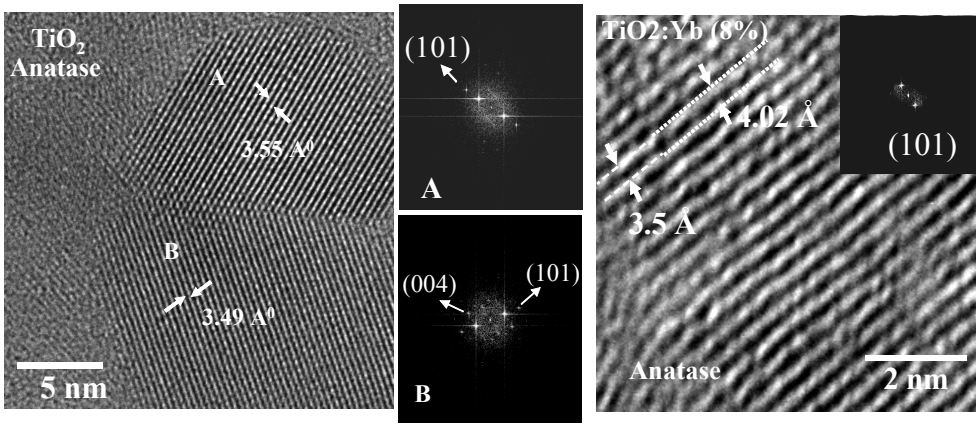

Figure 4. Typical HRTEM images of undoped (left) and 8% doped TiO_2 (right) nanoparticles along with their corresponding fast Fourier transforms.

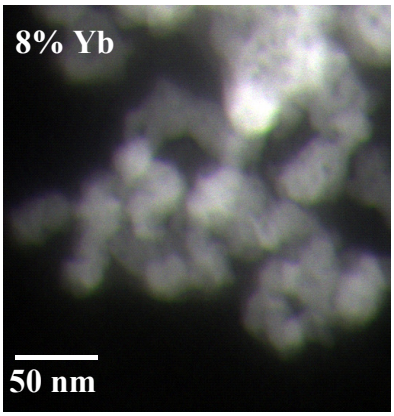

Figure 5. HAADF-STEM images of 8% Yb doped TiO_2 nanostructures. Bright contrast small Yb clusters are distributed inside the TiO_2 matrix.

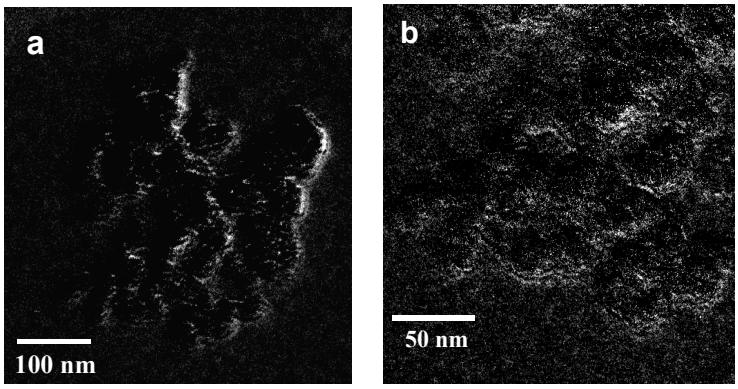

Figure 6. Ytterbium N-edge energy (185 eV) filtered images for 8% Yb doped TiO_2 nanoparticles showing Yb segregation towards surfaces.

Optical characterization through DRS

Optical properties of the powdered samples were studied by a Varian Cary 100 UV-Vis Diffuse Reflectance Spectrophotometer (DRS, spectrophotometer with DRA-CA-30I Diffuse Reflectance Accessoy). The absorption spectra of undoped and Yb-doped TiO_2 nanoparticles measured in diffuse reflectance mode are shown in figure 7. As can be seen, the absorption edges of Yb-doped nanoparticles were shifted to the lower energy region compared to undoped TiO_2. The largest redshift of the band edge occurred for the 0.5 % Yb-doped sample. The observation of band gap narrowing is similar to those reported by Li et al. [24] and Zhao et al. [9]. Using density functional theory calculations they have confirmed that some electronic states are introduced into the band gap of TiO_2 by lanthanide 4*f* electrons, which are located near the lower edge of conduction band to form new lowest unoccupied molecular orbital. Consequently, the electronic transition in Yb doped TiO_2 can occur from O 2*p* to Yb 4*f* instead of Ti 3*d* as in the case of pure TiO_2 which is reflected in overall band gap shrinkage in Yb-doped samples. For 8% doping the precipitation of excess Yb (not dissolved homogeneously in TiO_2 matrix) in the form of Yb clusters beneath the surface of the TiO_2 particles might be the reason for the lowest shift of the absorption edge in the visible energy region compared to 0.5 and 2% Yb doped samples.

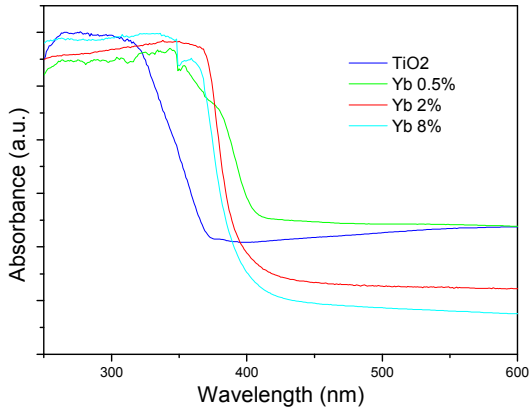

Figure 7. UV-Vis DRS absorption spectra of the undoped and Yb-doped TiO_2 nanoparticles.

Photocatalysis

Experimental set-up

The photocatalytic decomposition of MB (HYCEL, Mexico) was carried out using a homemade set-up. For each experimental run, 30 mg of TiO_2 catalyst was added to 250 ml of 15 ppm methylene blue aqueous solution and O_2 was bubbled through the reactiuon media dring the experiment. The solution was kept in the dark under stirring for 1 h and at every 10 min about 6 ml of the solution was extracted from the reaction medium for sampling in order to measure the adsorption of MB over the surface of TiO_2 nanoparticles. After this initial 1 h, the solution was irradiated under UV or visible light for another 5 h. Ultraviolet radiation was provided by a 15 W low pressure mercury vapor UV lamp (UVP-XX-15S) with short wavelength at 254 nm. The average light intensity was approximately 5.3 W m^{-2}. A fiber optic illuminator (Fiber-Lite, model 190) was used as a visible light source (> 400 nm, 30 W quartz halogen illumination system). After certain time of illumination, the catalyst was recovered from the reaction mixture by centrifugation, and the absorption spectra of the clear solutions were measured at 664 nm (λ_{max} for MB). The decolorization of MB was calculated from C/C_0; where C_0 and C are the concentrations of initial (original) and photodegraded MB solution.

Results and Discussion

The photocatalytic activity of undoped as well as Yb-doped TiO_2 nanoparticles was tested by UV light photodecomposition of MB, and the results are shown in figure 8. In general, the photocatalytic activity of pure TiO_2 is comparatively higher than that of the Yb doped samples under UV light. It has been found that the order of photocatalytic activity of Yb doped samples was as following: 0.5 < 2 < 8 < 0 mol %. The poor catalytic performance of the doped samples under UV light is due to the extension of their absorption edge into longer wavelength region. Figure 9 shows the normalized optical density change of MB solution at 664 nm under visible light irradiation (> 400 nm), photocatalyzed by undoped and Yb-doped TiO_2 nanoparticles. In general, photodegradation rate of MB was substantially improved for all the doped samples under visible light. It is found that the undoped TiO_2, a potential UV photocatalyst, reveals lowest visible light photocatalytic activity compared to the doped samples. The order of photocatalytic activity after 360 min of monitoring was: 0.5 > 2 > 8 > 0 mol %, suggesting that the Yb-doping enhances the catalytic performance of TiO_2 under visible light illumination, and the optimum doping concentration of Yb was 0.5 mol %.

The highest catalytic activity of 0.5 % Yb doped TiO_2 sample in comparison with the other samples is probably due to its absorption capacity in the extended visible region (Fig. 7). Though a high Yb doping increases the absorptive power of TiO_2 nanostructures, formation of Yb clusters beneath the particle surface enhances the recombination rate of photogenerated charge carriers, reducing their photocatalytic activity to some extent.

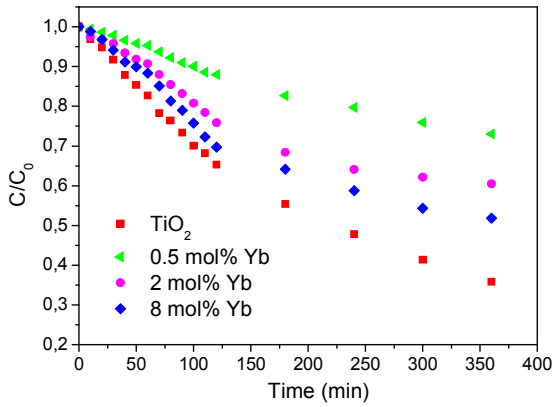

Figure 8. Photocatalytic degradation of methylene blue by undoped and ytterbium doped nanoparticles under UV light.

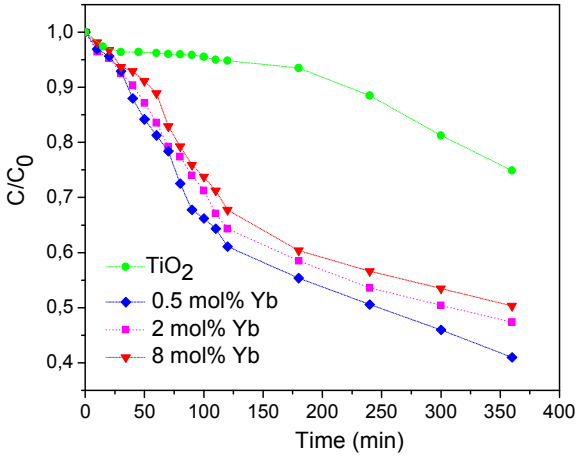

Figure 9. Photocatalytic degradation of methylene blue by undoped and Yb-doped TiO_2 nanoparticles under visible light.

Conclusions

Undoped and Yb doped TiO_2 nanoparticles of homogeneous size distribution were synthesized by controlled hydrolysis of titanium precursor using mild experimental conditions. All the doped and undoped nanoparticles remain in anatase phase on sintering them in nitrogen atmosphere at 550 ^{0}C. Though Yb doping does not have any particular effect on crystalline phase of TiO_2, it introduces lattice distortions, reducing the crystallinity and hindering the growth of the nanoparticles. Incorporated Yb in TiO_2 nanostructures form small clusters and precipitate below the particle surface, shifting the absorption edge towards visible wavelength range to some extent, and make them active for photocatalytic degradation of MB under visible light. However, the photocatalytic activity of TiO_2 nanoparticles might be hindered by incorporation Yb in excess amount.

Acknowledgements

The authors are grateful to Luis Rendon, IFUNAM, for acquiring electron microscopic images of the samples. The work was supported partially by CONACyT (Grant # 46269) and VIEP-BUAP (Grant # 93/EXC/2008-1), Mexico.

References

[1] X. Chen and S.S. Mao, Chem. Rev. Vol. 107 (2007), p. 2891
[2] J. Joo, S.G. Kwon, T. Yu, M. Cho, J. Lee, J. Yoon, T. Hyeon, J. Phys. Chem. B Vol. 109 (2005), p. 15297.
[3] H. Zhang and J.F. Banfield, J. Mater. Chem. Vol. 8 (1998), p. 2073
[4] R.R. Yeredla and H. Xu, *Nanotechnology*. Vol. 19 (2008), p. 055706
[5] H. Gerischer and A. Heller, J. Electrochem. Soc. Vol. 139 (1992), p.113
[6] K. Tanaka, M.F. Capule, and T. Hisanaga, Chem. Phys. Lett. Vol. 187 (1991), p. 73
[7] Q. Xiao, Z. Si, J. Zhang, C. Xiao, Z. Yu, G. Qiu, J. Mater. Sci. Vol. 42 (2007), p. 9194
[8] S.I. Shah, W. Li, C.P. Huang, O. Jung, and C. Ni, Proceedings of the National Academy of Science. Vol. 99 (2002), p. 6482
[9] Z. Zhao and Q. Liu, J. Phys. D: Appl. Phys. Vol. 41 (2008), p. 085417
[10] A.L. Linsebigler, G. Lu, J. T. Yates, Chem. Rev. Vol. 95 (1995), p. 735
[11] M. Kocher, T.K. Däubler, E. Harth, U. Scherf, A. Gügel, and D. Neher, Appl. Phys. Lett. Vol. 72 (1998) p. 650
[12] K.R. Gopidas M. Bohorquez, and P.V. kamat, J. Phys. Chem. Vol. 94 (1990), p. 6435
[13] W. Choi, A. Termin, MR Hoffman, J. Phys. Chem. Vol. 98 (1994), p. 13669
[14] D.H. Kim, S.I. Woo, S.H. Moon, H.D. Kim, B.Y. Kim, J.H. Cho, Y.G. Joh and E.C. Kim, Solid State Commun. Vol. 36 (2005), p. 554
[15] T. Umebayashi, T. Yamaki, H. Itoh, K. Asai, Appl. Phys. Lett. Vol. 81 (2002), p.454
[16] R. Asahi, T. Morikawa, T. Ohwaki, K. Aoki, Y. Taga, Science. Vol. 293 (2001), p. 269
[17] T. Tachikawa, S. Tojo, K. Kawai, M. Endo, M. Fujitsuka, T. Ohno, K. Nishijima, Z. Miyamoto, T. Majima, J. Phys. Chem. B. Vol. 108 (2004), p. 19299
[18] J-G Li, X. Wang, K. Watanabe, and T. Ishigaki, J. Phys. Chem. B. Vol. 110 (2006), p. 1121
[19] S. Jeon and P. Braun, Chem. Mater. Vol. 15 (2003), p. 1256
[20] Joint Comitee on Powder Diffraction Standard (JCPDS) cards No. 84-1286.
[21] X. Wei-Wei, D. Song-Yuan, H. Lin-Hua, L. Lin-Yun, W. Kong-Jia, Chin. Phys. Lett. Vol. 23(2006), p. 2288
[22] J. C. Yu, J. Lin, R.W.M. Kwak, J. Phys. Chem. B. Vol. 102 (1998), p. 5094
[23] S. Utsunomiya and R. C. Ewing, Environ. Sci. Technol. Vol. 37 (2003), p. 786
[24] W. Li, Y. Wang, H. Lin, S. Ismat Shah, C. P. Huang, D. J. Doren, S. A. Rykov, J. G. Chen and M. A. Barteau, Appl. Phys. Lett. Vol. 83 (2003), p. 4143

Journal of Nano Research Vol. 5
doi:10.4028/0-00000-029-9
Synthesis and Photocatalytic Activity of Yb Doped TiO₂ Nanoparticles under Visible Light
doi:10.4028/0-00000-029-9.193